Chapter 24

Lipopolysaccharide Membrane Building and Simulation

Sunhwan Jo, Emilia L. Wu, Danielle Stuhlsatz, Jeffery B. Klauda, Alexander D. MacKerell Jr., Göran Widmalm, and Wonpil Im

Abstract

While membrane simulations are widely employed to study the structure and dynamics of various lipid bilayers and membrane proteins in the bilayers, simulations of lipopolysaccharides (LPS) in membrane environments have been limited due to their structural complexity, difficulties in building LPS-membrane systems, and lack of the appropriate molecular force fields. In this work, as a first step to extend CHARMM-GUI *Membrane Builder* to incorporate LPS molecules and to explore their structures and dynamics in membrane environments using molecular dynamics simulations, we describe step-by-step procedures to build LPS bilayer systems using CHARMM and the recently developed CHARMM carbohydrate and lipid force fields. Such procedures are illustrated by building various bilayers of *Escherichia coli* R1.O6 LPS and the presentation of preliminary simulation results in terms of per-LPS area and density distributions of various components along the membrane normal.

Key words Lipid A, R1 core, O6 antigen, Bilayer, *E. coli*, Glycan, Molecular dynamics simulation

1 Introduction

Lipopolysaccharides (LPS), also known as endotoxins, cover the outer membrane of gram-negative bacteria [1–4]. They are amphiphilic compounds consisting of three regions: lipid A, a core oligosaccharide, and an O-antigen polysaccharide. Lipid A has acyl chains and anchors the LPS in the outer membrane. It is the bacterial lipid A component that is responsible for the toxic effects in mammalian cells by binding to Toll-like receptors with subsequent immunostimulation of the innate immune system and induction of inflammatory cytokines [5]. The core oligosaccharide is relatively conserved across species with only a few canonical structures (e.g., five in the case of *Escherichia coli*) consisting of about 10–12 monosaccharides. Finally, the O-antigen polysaccharide is made up of repeating units that are highly variable in sequence and structure.

In *E. coli*, about 190 different serogroups have been reported, and primary sequence information of more than half of their

Thomas Lütteke and Martin Frank (eds.), *Glycoinformatics*, Methods in Molecular Biology, vol. 1273,
DOI 10.1007/978-1-4939-2343-4_24,

O-antigen polysaccharides has been determined [6]. The number of repeats is usually on the order of 10–25, resulting in a molecular mass of up to 25 kDa [7], thereby creating a physical barrier and protective shield at the surface of the bacterium. In some cases, only "a single repeat" is observed leading to what is known as a semi-rough strain [8, 9]. These gram-negative bacteria may also co-express capsular [10] or exo-polysaccharides of even higher molecular mass, but this expression is dependent on, inter alia, environment and growth conditions.

In the LPS of *E. coli* (Fig. 1), the lipid A part consists of two glucosamine residues joined by a β-(1→6)-linkage, six *N*- and *O*-linked fatty acids for the canonical form, and phosphoester moieties. The inner core region has a few keto-deoxyoctulosonate (Kdo) residues, one of which is linked to the lipid A part, and L-*glycero*-D-*manno*-heptose (Hep) residues; in the outer core, half a dozen hexose residues are present. The O-antigen polysaccharide is likewise linked to one of the core sugars via a D-Glc*p*NAc or a D-Gal*p*NAc residue, and is built by repeating units usually consisting of three to six sugars that are either linear or branched, sometimes with more than one branch making the three-dimensional (3D) structure highly complex. The structural features of some of these polysaccharides are such that they can act by molecular mimicry [11], meaning that they imitate the glycoconjugate structures of the host that they invade or inhabit in a symbiotic manner. The three regions of the LPS have different functions, and it is essential to obtain information on their 3D structure and dynamics in order to understand the interactions of endotoxins in biological and biomedical systems.

While membrane simulations are widely employed to study the structure and dynamics of various lipid bilayers and membrane proteins in the bilayers (reviewed in refs. 12–17), simulations of LPS molecules in membrane environments [18, 19] have been limited due to its structural complexity, difficulties in building LPS membrane systems, and lack of appropriate molecular force field. We have developed CHARMM-GUI *Membrane Builder* [20, 21] to standardize and automate the building procedures of various lipid bilayers and membrane protein systems, and it is now possible to build and simulate various mixed bilayer systems (including cholesterol and multiple lipid types) with and without protein. In this work, as a first step to extend CHARMM-GUI *Membrane Builder* to incorporate LPS molecules and to explore their structures and dynamics in membrane environments using molecular dynamics (MD) simulations, we describe step-by-step procedures to build LPS bilayers using CHARMM [22] and the modified *Membrane Builder* procedure. For this work, we have added lipid A and new sugar types (e.g., core region Kdo and Hep residues) to the recently developed CHARMM carbohydrate and lipid force fields [23–28].

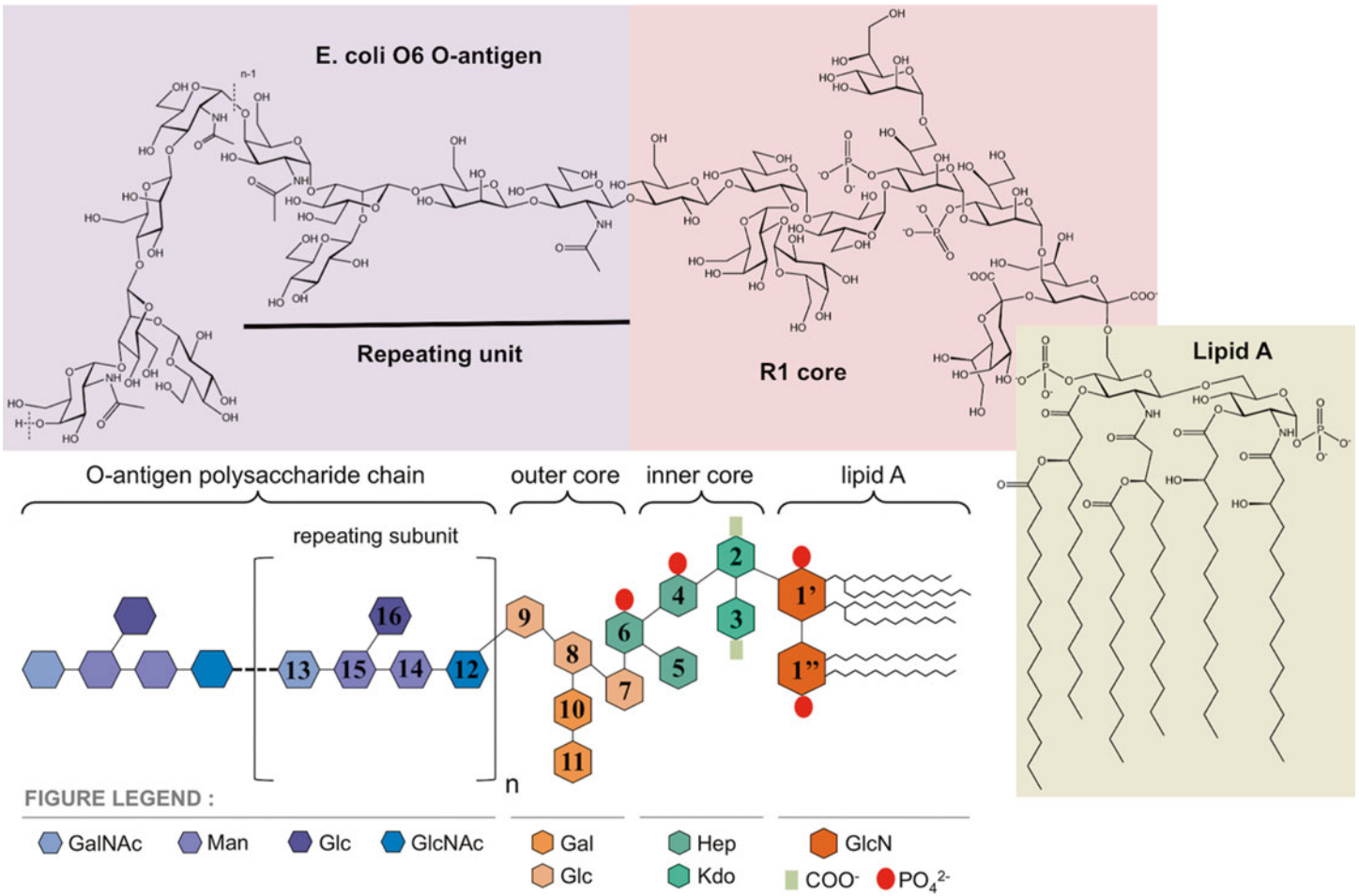

Fig. 1 Schematic of the lipopolysaccharide (LPS) of *E. coli* O6 having an R1 core. The LPS consists of three regions: lipid A, a core, and an O-antigen polysaccharide built of pentasaccharide repeating units. Note that the *N*-acetyl-D-glucosamine residue of the first repeating unit is ligated to the core via a β-linkage, whereas in the remaining part of the polysaccharide, it is joined via α-linkages to the subsequent repeating unit. The *dashed lines* indicate the repeating unit of the polymer and *n* describes the total number of repeating units in the O-antigen polysaccharide

A LPS molecule, *E. coli* R1 (core) O6 (antigen) [8], was used as an example in this study and described in the following section. In the Methods section (Subheading 3), the LPS bilayer building procedures are presented in terms of (1) generation of a LPS molecule, (2) building of LPS bilayer components, (3) their assembly, and (4) equilibration and production.

2 Materials

In this work, the 3D structure of *E. coli* R1.O6 LPS was built and simulated. The primary structure, i.e., sugar and lipid components, substituents, anomeric configurations, ring forms, substitution positions, and sequence of sugars, was previously determined using chemical and spectroscopic methods. The structural information comes from two studies. In the first study, the structure of the repeating unit of the O-antigen polysaccharide was determined [29]. In the second study, the semi-rough strain Nissle 1917 was investigated for lipid A, the core region, and one pentasaccharide unit [8]. As shown in Fig. 1, the lipid A structure of *E. coli* LPS consists of two D-glucosamine residues joined by a β-(1→6)-linkage, two monophosphoester groups at O1 and O4′, and six amide/ester-linked fatty acids which anchor the LPS in the outer membrane of the bacterium. The R1 core (most common core type reported for *E. coli*) of *E. coli* LPS has two Kdo residues and three Hep residues, two of which have a monophosphoester group at their respective O4 positions in the inner core (Fig. 1). Nonstoichiometric decoration with ethanolamine or glucosamine may also occur in this region. The outer core consists of five hexopyranoses, D-glucose, and D-galactose, all of which are α-linked, except for the terminal β-linked glucose (Fig. 1). The O-antigen polysaccharide of *E. coli* O6 LPS substitutes the O3 position of the terminal glucosyl residue in the core. The linkage between the reducing end sugar of the pentasaccharide and the core region has the β-configuration. This is in contrast to the corresponding α-(1→4)-linkage between the repeating units. Access to the semi-rough strain also facilitated determination of the biological repeating unit with a 3-substituted *N*-acetyl-D-glucosamine residue at the reducing end. The additional sugars in the repeating unit are two β-D-mannoses, an *N*-acetyl-α-D-galactosamine, leading to four sugars in the backbone of the polymer, and a β-D-glucose residue forming a branched structure via its (1→2)-linkage to the second mannose residue.

3 Methods

Figure 2 shows the overall building and simulation scheme of LPS bilayers that is comprised of five main steps. Each step is described in detail in Subheadings 3.1–3.4, and all the CHARMM inputs for the LPS5 system building (*see* below) with the topology and parameter files are available from http://im.compbio.ku.edu/Publications/download/MMB_tutorial.tgz.

3.1 Generation of a LPS Molecule (Step 1)

The first step [*step1_single.inp*] involves the generation of a single LPS molecule with proper sugar types, glycosidic linkages, and phosphorylation, starting from lipid A. For the *E. coli* R1.O6 LPS molecule (Fig. 1), each region (lipid A, R1 core, and O6 antigen) is generated and linked together in CHARMM. This generation step is shown explicitly below to illustrate the complexity of the sugar generation procedure with different glycosidic linkage types, in contrast to the generation of protein, which has identical peptide bonds between residues. Therefore, one needs to be very careful with the glycosidic linkage and sugar types.

Lipid A:

The molecular topology (LIPA) of Lipid A is initialized in CHARMM and assigned to a segment name of "L1".

```
READ SEQUENCE LIPA 1
GENERATE L1 FIRST NONE LAST NONE SETUP WARN
```

R1 core:

The sugar residues of the core are initialized and a segment name of "C1" is assigned. Note that the R1 core consists of ten residues and the sequence of the residues is not arranged in a consecutive manner due to branches in the sequence. Once initialized, each residue is connected by the appropriate glycosidic linkages using PATCH commands.

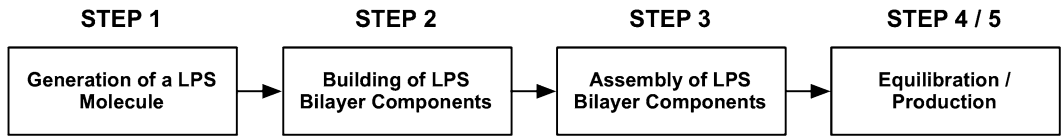

Fig. 2 Overall building and simulation procedure of a LPS bilayer

```
READ SEQUENCE CARD
* LPS core
*
10
KDOA KDOA HEPA HEPA HEPA
AGLC AGLC BGLC AGAL AGAL
GENERATE C1 FIRST NONE LAST NONE SETUP WARN
PATCH KD24E C1 1 C1 2 SETUP WARN
PATCH KH15A C1 1 C1 3 SETUP WARN
PATCH 13AB C1 3 C1 5 SETUP WARN
PATCH HH17A C1 5 C1 4 SETUP WARN
PATCH 13AB C1 5 C1 6 SETUP WARN
PATCH 13AB C1 6 C1 7 SETUP WARN
PATCH 13BB C1 7 C1 8 SETUP WARN
PATCH 12AB C1 7 C1 9 SETUP WARN
PATCH 12AB C1 9 C1 10 SETUP WARN
PATCH PH4B C1 3 SETUP WARN ! phosphorylation
PATCH PH4B C1 5 SETUP WARN ! phosphorylation
```

Lipid A – R1 link:

The core (segment "C1") and lipid A (segment "L1") segments are joined together using a PATCH command.

```
PATCH LK26A L1 1 C1 1 SETUP WARN
AUTOGENERATE ANGLE DIHE
```

O6 antigen:

The O-antigen is composed of a varying number of the repeating units, where each one consists of five residues in the case of O6. In CHARMM, one can take an advantage of the scripting facility in the input level, which allows writing flexible input scripts that can generate a LPS with different number of repeating units without changing the input. In the first half of the input, the first repeating unit of O6 antigen is generated and a segment name of "O1" is assigned. In the second part of the input (starting from the LABEL command), the input goes into a loop and repeats the command in between LABEL and GOTO commands until the condition is met (until the variable "I" is less than the variable "Noantigen," which is an input number of the O-antigen unit). Inside the loop, an additional repeating unit is generated and different segment names are assigned ("O2", "O3", …). Note that "@I" represents the value of the variable "I".

```
              READ SEQUENCE CARD
* LPS o-antigen unit
*
5
BGLCNA AGALNA BMAN BMAN BGLC
GENERATE O1 FIRST NONE LAST NONE SETUP WARN
PATCH 13BB O1 1 O1 3 SETUP WARN
PATCH 14BB O1 3 O1 4 SETUP WARN
PATCH 13AB O1 4 O1 2 SETUP WARN
PATCH 12BA O1 4 O1 5 SETUP WARN
CALC I =2
LABEL DOGENER
READ SEQUENCE CARD
* LPS o-antigen unit
*
5
AGLCNA AGALNA BMAN BMAN BGLC
GENERATE O@I FIRST NONE LAST NONE SETUP WARN
PATCH 13BB O@I 1 O@I 3 SETUP WARN
PATCH 14BB O@I 3 O@I 4 SETUP WARN
PATCH 13AB O@I 4 O@I 2 SETUP WARN
PATCH 12BA O@I 4 O@I 5 SETUP WARN
INCREASE I BY 1
IF I .LE. @nOANTIGEN GOTO DOGENER
```

R1 – O6 link:

The core structure and the first unit of O-antigen are connected here.

```
PATCH 13BB c1 8 o1 1 SETUP WARN
```

O6 – O6 link:

Each repeating unit of O-antigen is connected sequentially here.

```
CALC I =2

LABEL DOPATCH

CALC J=@I - 1

PATCH 14AA o@J 2 o@I 1 SETUP WARN

INCREASE I BY 1

IF I .LE. @nOANTIGEN GOTO DOPATCH
```

Like other typical lipid molecules, LPS molecules in a membrane environment may have various conformations, and unfortunately, no information of average glycosidic bond dihedral angles or their probable distributions are currently available. This implies that the initial LPS 3D structures need to be modeled properly to build a LPS bilayer, and sufficient conformational sampling of the LPS molecules using MD simulations would be necessary to obtain representative (or an ensemble of) LPS structures in the membrane environment. Initial coordinates of the LPS molecule were assigned using internal coordinate information of common glycosidic dihedral angle values (*see* Table 1) through the "IC BUILD" command in CHARMM. To improve sampling and study the impact of chain length of the O-antigen polysaccharide, we have built four different *E. coli* R1.O6 LPS molecules and a corresponding bilayer for each LPS. For simplicity, they are denoted as LPS0 (lipid A+R1 core),

Table 1
Initial glycosidic torsion angles

Glycosidic linkage[a]		Glycosidic torsion angle[b]			
		ϕ	ψ	ω	ε
$1' \rightarrow 1''$	β-(1→6)	−65	−130	60	
$2 \rightarrow 1'$	α-(2→6)	68	180	162	
$3 \rightarrow 2$	α-(2→4)	60	−86		
$4 \rightarrow 2$	α-(1→5)	22	−125		
$5 \rightarrow 4$	α-(1→3)	65	−141		
$6 \rightarrow 5$	α-(1→7)	71	120	−41	−120
$7 \rightarrow 5$	α-(1→3)	65	−141		
$8 \rightarrow 7$	α-(1→3)	65	−141		
$9 \rightarrow 8$	α-(1→2)	87	115		
$10 \rightarrow 9$	α-(1→2)	87	115		
$11 \rightarrow 9$	β-(1→3)	−130	−130		
$12 \rightarrow 11$	β-(1→3)	−130	−130		
$13 \rightarrow 12$	β-(1→3)	−130	−130		
$14 \rightarrow 13$	β-(1→4)	−130	82		
$15 \rightarrow 14$	β-(1→2)	−168	−130		
$16 \rightarrow 14$	α-(1→3)	65	−141		

[a]Residue number is used for monosaccharides in the LPS molecule (*see* Fig. 1)
[b]The following glycosidic torsion angle definitions are adopted: $\phi = O_5'\text{-}C_1'\text{-}O_x\text{-}C_x$, $\psi = C_1'\text{-}O_x\text{-}C_x\text{-}C_{(x\text{-}1)}$, $\omega = O_x\text{-}C_x\text{-}C_{(x\text{-}1)}\text{-}C_{(x\text{-}2)}$, and $\varepsilon = C_x\text{-}C_{(x\text{-}1)}\text{-}C_{(x\text{-}2)}\text{-}C_{(x\text{-}3)}$, whereas for the (2→6)- and (2→4)- linkages $\phi = O_6'\text{-}C_2'\text{-}O_x\text{-}C_x$, $\psi = C_2'\text{-}O_x\text{-}C_x\text{-}C_{(x\text{-}1)}$, $\omega = O_x\text{-}C_x\text{-}C_{(x\text{-}1)}\text{-}C_{(x\text{-}2)}$

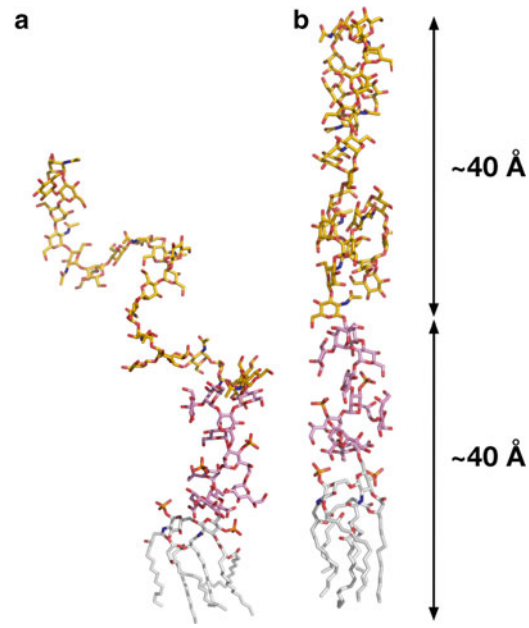

Fig. 3 3D structures of a LPS5 (lipid A + R1 core + five units of O6 antigen) single molecule, generated by (**a**) CHARMM IC BUILD and (**b**) Langevin dynamics with cylindrical restraints: lipid A (*gray*), R1 core (*pink*), and O6-antigen (*yellow*)

LPS5 (lipid A + R1 core + 5 units of O6 antigen), LPS10 (lipid A + R1 core + 10 units of O6 antigen), and LPS20 (lipid A + R1 core + 20 units of O6 antigen). Figure 3a shows the 3D structure of a single LPS5 molecule.

Any LPS initial structures generated by "IC BUILD" may not be linear as shown in Fig. 3a, and any nonlinear LPS structure can cause severe bad contacts when they are assembled to form a membrane. Therefore, to make the building procedure general for any types of LPS molecules, the following procedures are used to make each individual LPS molecule to be cylindrical [*step1_ld.inp*].

1. Orient each LPS molecule along the *Z*-axis and place phosphorus atoms (P_A and P_B) of lipid A at $Z = 20$ Å; the *Z*-axis is parallel to the bilayer normal.
2. Perform Langevin dynamics (LD) with the oriented LPS molecule using a cylindrical restraint potential to restrain the LPS molecule to be cylindrical in shape.

We ran a total of 12 sequential LD simulations. Each run was 10 ps, and the target radius for the cylindrical restraint potential starting from a radius of 16 Å was reduced by 1 Å in each subsequent simulation to make the final LPS molecule confined in a cylinder with a radius of 8 Å. A radius of 8 Å roughly corresponds to a per-lipid area of 200 Å^2 that was used for an initial guess of the LPS molecule surface area. To avoid any severe bad contacts during

the membrane assembly, we used a slightly larger area (200 Å^2) than 180 Å^2; 180 Å^2 is an estimate based on an assumption from DMPC that each of the 6 acyl chains in lipid A covers about ~30 Å^2 [30]. The LPS area in the membrane would be converged during the NPT (constant pressure and temperature) dynamics for equilibration and production (Step 4/5). The resulting LPS5 structure after the LD simulations is shown in Fig. 3b.

3.2 Building of LPS Bilayer Components (Step 2)

The most critical step in creation of an LPS bilayer is the proper assembly of the individual LPS components into the membrane system, which includes the bilayer itself, ions, and water. First, LPS bilayers composed of 50 LPS0, LPS5, LPS10, or LPS20 monomers (25 LPSs in each leaflet) were made through the following rigid-body search procedure [*step2_bilayer.inp*].

1. The $X\Upsilon$ centers of P_A and P_B (two phosphorus atoms of lipid A) were initially placed in a 5×5 square grid with random rotations along the Z-axis in one leaflet. The grid spacing was based on an initial surface area of 200 Å^2/LPS.
2. The initial Z position of lipid A P_A and P_B was set to 20 Å.
3. To remove bad contacts, a systematic translation and rotational rigid-body search was performed for each LPS molecule: translation with ~1.1 Å spacing for ±2.2 Å search from each LPS's $X\Upsilon$ position (5 moves in the X and Υ directions, respectively) and rotation with 11° interval for 360° (32 moves). A bad contact is defined when a heavy atom–heavy atom distance is less than 2.5 Å.
4. The search continued until the average number of bad contacts per lipid reached a minimum. 5 independent systems were made for each LPS molecule using different initial random number seeds, and the average number of bad contacts per lipid was 0 (LPS0), 0.03 (LPS5), 0.2 (LPS10), and 0.4 (LPS20). Simulations of multiple independent systems provide better sampling and one can also check the simulation convergence.
5. To build a bilayer, the lower leaflet was generated by 180° rotation of the upper leaflet with respect to the X-axis. Accordingly, the bilayer center is located at $Z = 0$. The resulting structure of a LPS5 bilayer is shown in Fig. 4a.

The next step is to generate ions [*step2_ions.inp*]. The total charge of *E. coli* lipid A and R1 core is $-10e$ and the O_6-antigen segment is neutral. Ca^{2+} was used to neutralize the lipid A and the core, i.e., 125 Ca^{2+} ions in each leaflet. 150 mM KCl was used for bulk ionic solution, and the number of KCl ions was determined by the system area times the 10 Å bulk region (along the Z-axis), i.e., 10 K^+ and Cl^- ions. To obtain initial positions of ions, we performed 2000 steps of Monte Carlo (MC) simulations for Ca^{2+} ions and 2000 steps of MC simulations for K^+ and Cl^- ions. LPS-ion

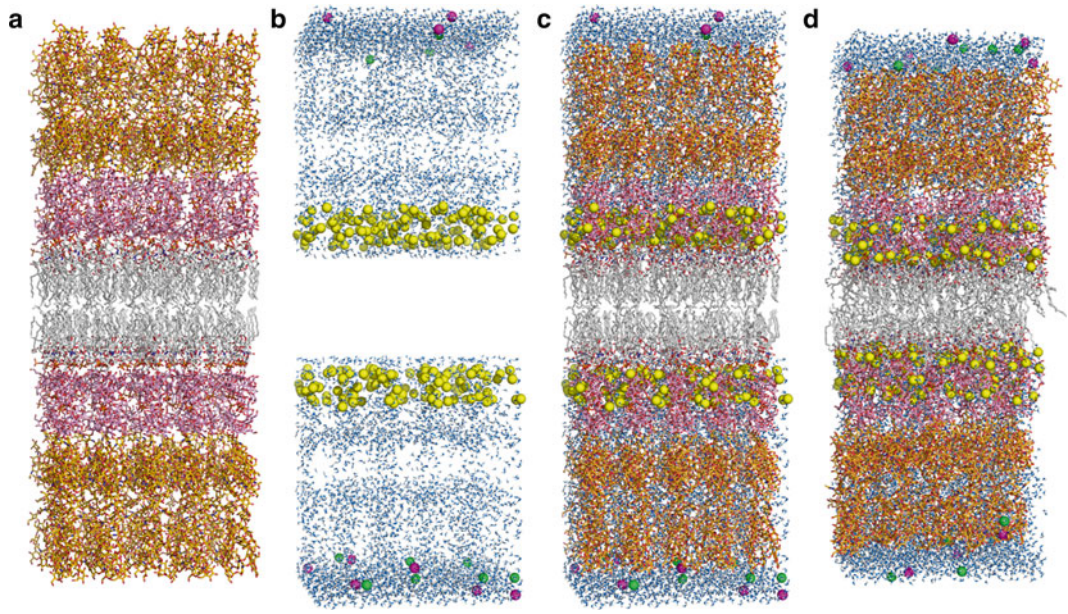

Fig. 4 LPS5 bilayer simulation system. (**a**) An initial bilayer assembly through the rigid-body search to minimize the number of bad contacts. (**b**) Initial positions of water molecules (*light blue*) and ions (Ca^{2+}: *yellow*, K^{+}: *magenta*, and Cl^{-}: *green*). (**c**) An initially assembled structure (A + B). (**d**) A structure after equilibration

interaction energies were calculated using a primitive model that included the Coulombic interaction scaled by a dielectric constant of 80 and van der Waals interaction. During the MC runs, Ca^{2+} ions (125 for each leaflet) were restricted to the lipid A and core region, and K^{+} and Cl^{-} ions to the bulk region. The resulting ion positions in a LPS5 bilayer are shown in Fig. 4b. Finally, a water box was made to solvate the LPS bilayer systems in the next step [*step2_waterbox.inp*]. The water box had a dimension of the system area (XY) times 20 Å (Z).

3.3 Assembly of LPS Bilayer Components (Step 3)

This step assembles the components and solvates the system per following procedure [*step3_assembly.inp*].

1. LPS bilayer and ions were assembled as described in Subheading 3.2.
2. The water box was duplicated and sequentially overlaid onto the LPS bilayer and ions from $Z = +15$ Å to Z_{max} and from $Z = -15$ Å to Z_{min}; Z_{max} is defined by the maximum Z position of the LPS molecules in the upper leaflet plus the 10 Å bulk water region, and Z_{min} is defined by the minimum Z position of the LPS molecules in the lower leaflet minus the 10 Å bulk water region. Any water molecule whose oxygen atom had a distance less than 2.8 Å from any LPS non-hydrogen atoms or ions was removed during the sequential overlays. The resulting structure of a fully hydrated LPS5 bilayer is shown in Fig. 4c.

Table 2
Various force constants applied during the equilibration steps

Step	4.1	4.2	4.3	4.4	4.5	4.6	4.7	4.8	4.9	4.10
k_{water}	2.5	2.5	1	1	0.5	0.1	0	0	0	0
k_{head}	2.5	2.5	1	1	0.5	0.1	0	0	0	0
k_{tail}	2.5	2.5	1	1	0.5	0.1	0	0	0	0
k_{chiral}	250	100	50	50	25	5	0	0	0	0
k_{ring}	250	200	150	100	100	50	50	50	25	25
$k_{bilayer}$	0	0	0	0	0	0	1	1	1	1

k_{water} is the force constant [in kcal/(mol·Å^2)] for the repulsive planar restraints to prevent water from entering into the membrane hydrophobic region ($|Z| < 12$ Å)
k_{head} is the force constant [in kcal/(mol·Å^2)] for the planar restraints to hold the position of lipid A P_A and P_B along the Z-axis ($Z = 20$ Å for the upper leaflet and $Z = -20$ Å for the lower leaflet)
k_{tail} is the force constant [in kcal/(mol·Å^2)] for the planar restraints to keep the last atoms of lipid A acyl chains in ($|Z| < 5$ Å)
k_{chiral} is the force constant [in kcal/(mol·rad^2)] for the dihedral restraints to maintain the correct chirality in the lipid A
k_{ring} is the force constant [in kcal/(mol·rad^2)] for the dihedral restraints to maintain the chair conformation of sugars
$k_{bilayer}$ is the force constant [in kcal/(mol·Å^2)] for the planar restraint to hold the position of lipid A molecules at $Z = 0$

3. 5 independent systems were built for each LPS bilayer type by repeating the above steps with different initial random number seeds. The number of atoms in each bilayer system is ~48,000 (LPS0), ~84,000 (LPS5), ~136,000 (LPS10), and ~225,000 (LPS20). Due to the system size, we did not herein perform equilibration and production for the LPS20 system.

3.4 Equilibration and Production (Step 4/5)

After a complex LPS bilayer system is assembled, simulations to equilibrate the system must be performed to relax the initial system. In this work, we have modified/extended the equilibration steps used in the current CHARMM-GUI *Membrane Builder* for the LPS bilayer system. As shown in Table 2, to assure gradual equilibration of the assembled system, various restraints are applied to the LPS and water molecules, and the restraint forces are gradually reduced during the equilibration [*step4.*[*1–15*]*_equilibration.inp*]. In addition, to warrant the successful equilibration, i.e., to avoid instability of the dynamics integrator during equilibration, NVT dynamics (constant volume and temperature) were used for the first and second steps and NPT (constant temperature and pressure) dynamics for the rest at 310 K. Each equilibration run was 25,000 steps (1-fs timestep in steps 1–3 and 2-fs timestep in steps 4–10). The equilibrated structure of a fully hydrated LPS5 bilayer is shown in Fig. 4d. Note that there is no unique equilibration procedure, but the aforementioned equilibration steps (also in

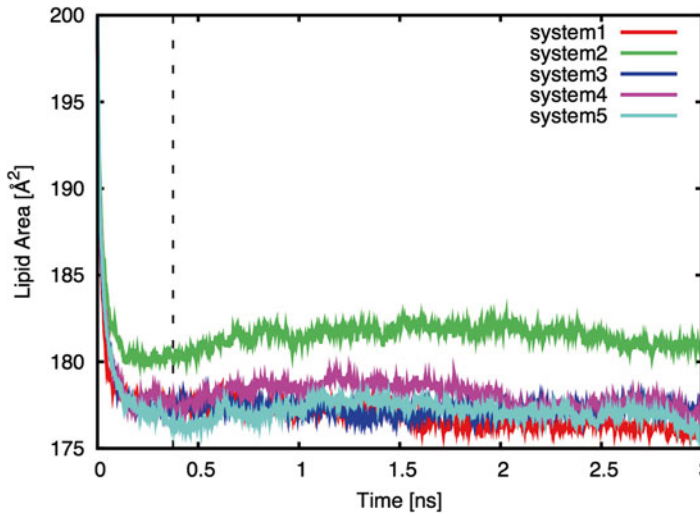

Fig. 5 Time-series of per-LPS area in the five independent LPS5 bilayer systems color coded for each run. The *dotted line* represents the end of the NPT equilibration (step 4.3–step 4.10)

Table 2) were optimized through trial-and-error. It also needs to be emphasized that the correct nonbonded atom–atom interaction schemes appropriate for lipid bilayers, as described in Klauda et al. [26], should be applied in the equilibration as well as production simulations.

The MD production run is basically the continuation of the (equilibration) simulations without any restraints [*step5_production.inp*]. However, most membrane MD simulation runs require extended simulation times to fully equilibrate the systems even after the (proposed) equilibration steps. In the LPS bilayer simulation case, we found that it was necessary to keep the restraint potential for the $^4C_1$ sugar conformation (k_{ring}). This was required to avoid the sugar conformation switching due to unfavorable interactions with the surrounding environment. Figure 5 shows the time-series of per-LPS area in the 5 independent LPS5 systems (including the equilibration steps), and Fig. 6 shows the heavy atom distributions of the systems along the *Z*-axis. While Fig. 5 shows that the surface area per LPS relaxes relatively quickly, it does not indicate that the system is adequately converged. Other properties such as the sampling of dihedrals in various parts of the LPS molecules, water or ion distributions, and so on should be monitored. And it should be emphasized that the definition of convergence is based on the properties of the system being monitored. The results in Fig. 6, while not converged, are presented to illustrate the type of information one can obtain from the LPS bilayer simulations. Given the complexity of LPS bilayers and the difficulty of experimental methods to elucidate atomic details of these types of biological systems, MD simulations offer a unique window to understand the structure and dynamics of these complex systems.

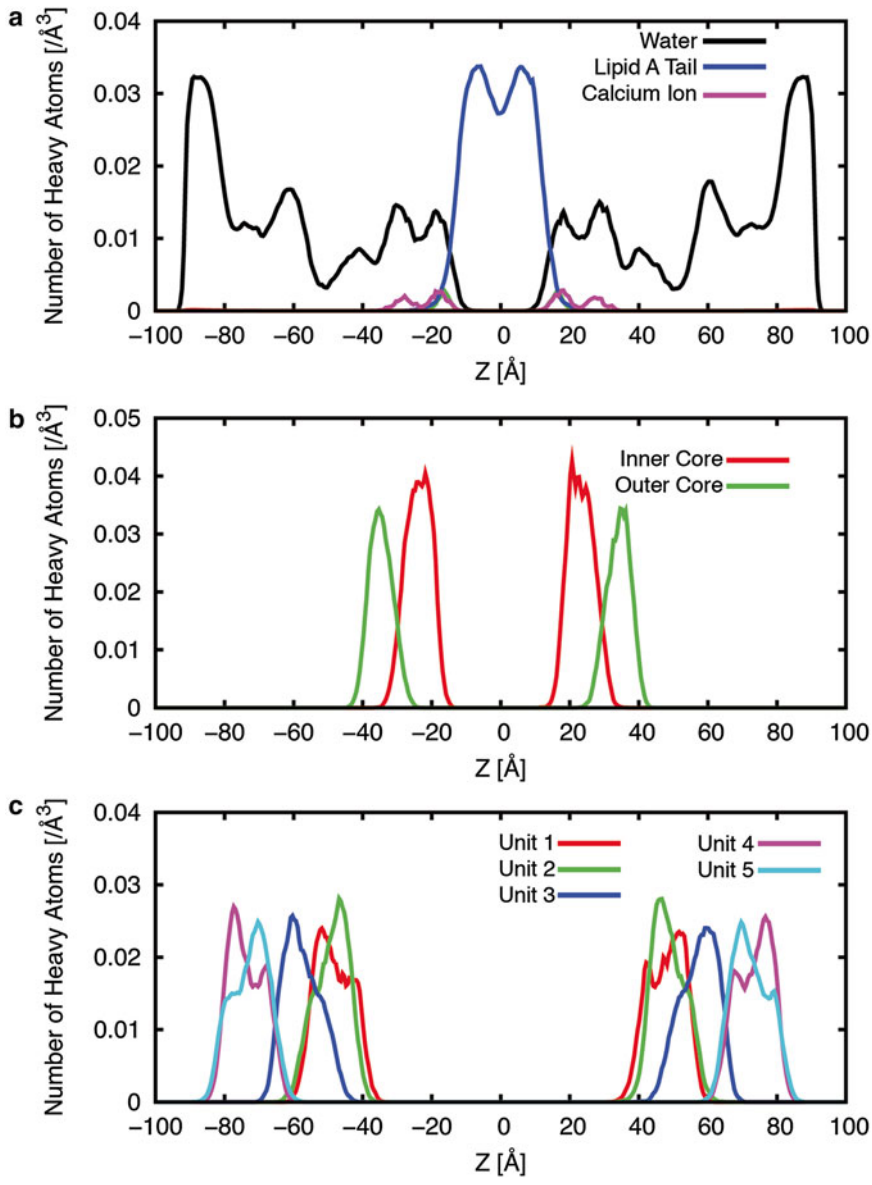

Fig. 6 Heavy atom distributions of the LPS5 systems along the Z-axis. (**a**) Water, lipid A, and calcium ion. (**b**) The inner and outer core. (**c**) Five repeating O-antigen units. The distributions were averaged over the five independent systems over the production time (2.6 ns, cf. Fig. 5)

4 Conclusions

We have described the detailed procedure to build the *E. coli* R1.O6 LPS bilayer systems. While the LPS molecules only exist in the outer leaflet of the outer membrane of *E. coli*, we used a bilayer system simply to increase the conformational sampling during MD simulations. Note that while not explicitly described, building an

asymmetric membrane system should be relatively easy. We expect that long simulations (more than 100 ns) will be required for these complex LPS systems and a critical validation of the bilayer properties obtained from the simulations will be necessary. To this end, NMR studies on the O-antigen using ^{1}H,^{1}H-NOESY experiments and ultimately NMR data on the complete LPS molecule need to be measured in order to compare with and validate the MD simulations of these LPS bilayers. We also plan to incorporate the LPS membrane building procedure in CHARMM-GUI *Membrane Builder* in the future for its wider usage along with the ability to build the biologically relevant asymmetric bilayer.

This book chapter was submitted in December, 2011. Since then, we have made significant progresses that resulted in two publications [31, 32]. Nonetheless, we believe that the building procedure described here would be useful (or provide a guideline) to the readers who are interested in building these complex systems.

Acknowledgements

This work was supported by the University of Kansas General Research Fund allocation #2301388-003, Kansas-COBRE NIH P20 RR-17708, TeraGrid resources provided by Purdue University (NSF OCI-0503992) (to W.I.) and grants from the NIH (GM070855) (to A.D.M.), and from the Swedish Research Council and the Stockholm Center for Biomembrane Research/ Swedish Foundation for Strategic Research (to G.W.).

References

1. Brade H, Opal SM, Vogel SN, Morrison DC (eds) (1999) Endotoxin in health and disease. Marcel Dekker, NY
2. Knirel YA, Valvano, MA (eds) (2011) Bacterial polysaccharides. Structure, chemical synthesis, biogenesis and interaction with host cells. Springer-Verlag, Wien
3. Silipo A, Castro DC, Lanzetta R, Parrilli M, Molinaro A (2010) Lipopolysaccharides. In: König H, Claus H, Varma A (eds) Prokaryotic cell wall compounds. Springer, Berlin, pp 133–153
4. Wang X, Quinn PJ (2010) Endotoxins: lipopolysaccharides of gram-negative bacteria. In: Wang X, Quinn PJ (eds) Endotoxins: structure, function and recognition, subcellular biochemistry. Springer, Dordrecht, pp 3–25
5. Akira S, Uematsu S, Takeuchi O (2006) Pathogen recognition and innate immunity. Cell 124:783–801
6. Stenutz R, Weintraub A, Widmalm G (2006) The structures of Escherichia coli O-polysaccharide antigens. FEMS Microbiol Rev 30:382–403
7. Linnerborg M, Weintraub A, Widmalm G (1999) Structural studies utilizing ^{13}C-enrichment of the O-antigen polysaccharide from the enterotoxigenic Escherichia coli O159 cross-reacting with Shigella dysenteriae type 4. Eur J Biochem 266:246–251
8. Grozdanov L, Zahringer U, Blum-Oehler G, Brade L, Henne A, Knirel YA, Schombel U, Schulze J, Sonnenborn U, Gottschalk G, Hacker J, Rietschel ET, Dobrindt U (2002) A single nucleotide exchange in the wzy gene is responsible for the semirough O6 lipopolysaccharide phenotype and serum sensitivity of Escherichia coli strain Nissle 1917. J Bacteriol 184: 5912–5925

9. Knirel YA, Widmalm G, Senchenkova SN, Jansson PE, Weintraub A (1997) Structural studies on the short-chain lipopolysaccharide of Vibrio cholerae O139 Bengal. Eur J Biochem 247:402–410
10. Whitfield C (2006) Biosynthesis and assembly of capsular polysaccharides in Escherichia coli. Annu Rev Biochem 75:39–68
11. Moran AP, Knirel YA, Senchenkova SN, Widmalm G, Hynes SO, Jansson PE (2002) Phenotypic variation in molecular mimicry between Helicobacter pylori lipopolysaccharides and human gastric epithelial cell surface glycoforms—acid-induced phase variation in Lewis(X) and Lewis(Y) expression by H. Pylori lipopolysaccharides. J Biol Chem 277:5785–5795
12. Ash WL, Zlomislic MR, Oloo EO, Tieleman DP (2004) Computer simulations of membrane proteins. Biochim Biophys Acta 1666:158–189
13. Gumbart J, Wang Y, Aksimentiev A, Tajkhorshid E, Schulten K (2005) Molecular dynamics simulations of proteins in lipid bilayers. Curr Opin Struct Biol 15:423–431
14. Lindahl E, Sansom MSP (2008) Membrane proteins: molecular dynamics simulations. Curr Opin Struct Biol 18:425–431
15. Pastor RW, MacKerell AD (2011) Development of the CHARMM force field for lipids. J Phys Chem Lett 2:1526–1532
16. Feller SE (2000) Molecular dynamics simulations of lipid bilayers. Curr Opin Colloid Interface Sci 5:217–223
17. Stansfeld PJ, Sansom MSP (2011) Molecular simulation approaches to membrane proteins. Structure 19:1562–1572
18. Lins RD, Straatsma TP (2001) Computer simulation of the rough lipopolysaccharide membrane of Pseudomonas aeruginosa. Biophys J 81:1037–1046
19. Straatsma TP, Soares TA (2009) Characterization of the outer membrane protein OprF of Pseudomonas aeruginosa in a lipopolysaccharide membrane by computer simulation. Proteins 74:475–488
20. Jo S, Kim T, Im W (2007) Automated builder and database of protein/membrane complexes for molecular dynamics simulations. PLoS One 2:e880
21. Jo S, Lim JB, Klauda JB, Im W (2009) CHARMM-GUI membrane builder for mixed bilayers and its application to yeast membranes. Biophys J 97:50–58
22. Brooks BR, Brooks CL, Mackerell AD Jr, Nilsson L, Petrella RJ, Roux B, Won Y, Archontis G, Bartels C, Boresch S, Caflisch A, Caves L, Cui Q, Dinner AR, Feig M, Fischer S, Gao J, Hodoscek M, Im W, Kuczera K, Lazaridis T, Ma J, Ovchinnikov V, Paci E, Pastor RW, Post CB, Pu JZ, Schaefer M, Tidor B, Venable RM, Woodcock HL, Wu X, Yang W, York DM, Karplus M (2009) CHARMM: the biomolecular simulation program. J Comput Chem 30:1545–1614
23. Guvench O, Greene SN, Kamath G, Brady JW, Venable RM, Pastor RW, Mackerell AD Jr (2008) Additive empirical force field for hexopyranose monosaccharides. J Comput Chem 29:2543–2564
24. Guvench O, Hatcher E, Venable RM, Pastor RW, MacKerell AD Jr (2009) CHARMM additive all-atom force field for glycosidic linkages between hexopyranoses. J Chem Theory Comput 5:2353–2370
25. Hatcher E, Guvench O, MacKerell AD Jr (2009) CHARMM additive all-atom force field for aldopentofuranoses, methyl-aldopentofuranosides, and fructofuranose. J Phys Chem B 113:12466–12476
26. Klauda JB, Venable RM, Freites JA, O'Connor JW, Tobias DJ, Mondragon-Ramirez C, Vorobyov I, MacKerell AD Jr, Pastor RW (2010) Update of the CHARMM all-atom additive force field for lipids: validation on six lipid types. J Phys Chem B 114: 7830–7843
27. Guvench O, Mallajosyula SS, Raman EP, Hatcher E, Vanommeslaeghe K, Foster TJ, Jamison FW 2nd, Mackerell AD Jr (2011) CHARMM additive all-atom force field for carbohydrate derivatives and its utility in polysaccharide and carbohydrate-protein modeling. J Chem Theory Comput 7:3162–3180
28. Mallajosyula SS, Guvench O, Hatcher ER, Mackerell AD Jr (2012) CHARMM additive all-atom force field for phosphate and sulfate linked to carbohydrates. J Chem Theory Comput 8:759–776
29. Jansson PE, Lindberg B, Lönngren J, Ortega C, Svenson SB (1984) Structural studies of the Escherichia coli O-antigen 6. Carbohydr Res 131:277–283
30. Klauda JB, Kucerka N, Brooks BR, Pastor RW, Nagle JF (2006) Simulation-based methods for interpreting x-ray data from lipid bilayers. Biophys J 90:2796–2807
31. Wu EL, Engström O, Jo S, Stuhlsatz D, Yeom MS, Klauda JB, Widmalm G (2013) Molecular dynamics simulation and NMR spectroscopy studies of E. coli lipopolysaccharide structure and dynamics. Biophys. J. 105:1444–1455
32. Wu EL, Fleming P, Yeom MS, Widmalm G, Klauda JB, Fleming KG, Im W (2014) E. Coli Outer Membrane and Interactions with OmpLA. Biophys. J. 106:2493–2502